

Lasers in Manufacturing Conference 2017

Femtosecond laser micropatterning of diamond-like nanocomposite coatings to improve friction on the microscale

Sergei Pimenov^{a,*}, Evgeny Zavedeev^a, Natalia Arutyunyan^a, Olga Zilova^b,
Mikhail Shupegin^b, Beat Jaeggi^c, Beat Neuenschwander^c

^aGeneral Physics Institute, Vavilov str. 38, Moscow 119991, Russia

^bNational Research University "Moscow Power Engineering Institute", Krasnokazarmennaja str. 14, Moscow 111250, Russia

^cBern University of Applied Sciences, Institute for Applied Laser, Photonics and Surface Technologies ALPS, Pestalozzistrasse 20, Burgdorf CH-3400, Switzerland

Abstract

We report on femtosecond laser micropatterning of diamond-like nanocomposite (DLN) coatings (SiO_x containing diamond-like carbon films) and investigation of the frictional properties of laser-patterned films on the nano and microscale. The DLN films of 2-3 μm thickness were irradiated using a femtosecond laser ($\lambda=1030$ nm, $\tau=320$ fs) at low fluences (below the single-pulse damage threshold) corresponding to the conditions of surface graphitization and incipient ablation developing during multipulse irradiation. The low-fluence multipulse irradiation was applied to produce periodic linear micropatterns (graphitized strips of <10 μm width and 20 μm period) on the DLN films. Microfriction properties of the laser-patterned films were studied using atomic force microscopy (AFM) in the lateral force mode. It was found that transition from nano to microscale (by increasing an AFM tip radius from 10 nm to 1.5 μm) was characterized by significant changes in the friction behaviour of laser-patterned films, demonstrating much lower friction forces within laser-irradiated areas than on the original film. The laser-patterned surface was found to exhibit changes in the wettability due to enlarged hydrophobicity of laser-graphitized surface. This resulted in a strong influence of capillary forces on the friction forces under the 'nano' loads and lowering of the friction forces on the laser-modified surface. The relative role of laser-induced surface modifications (graphitization, spallation, ablation, nanostructuring) in the observed microfriction behaviour is discussed.

Keywords: Diamond-like nanocomposite film; femtosecond laser; graphitization; ablation; micropatterning; friction force microscopy

* Corresponding author. Tel.: +7-499-503 8315.
E-mail address: pimenov@nsc.gpi.ru.

1. Introduction

Lasers are widely used in micro and nanoprocessing of materials to produce surface patterns and generate new material properties required for various applications in optics, photonics, tribology, and other fields [Konov, 2012; Mottay et al., 2016]. In tribology, laser surface micropatterning (laser surface texturing) is known as an effective technique to control friction and wear properties of hard materials and coatings under different sliding conditions [Etsion, 2005] when the produced surface micropatterns may act as micro-reservoirs for lubricants and traps for wear particles. Tribological behaviour of hard diamond-like carbon (DLC) films can additionally benefit from the laser-induced structure modification (graphitization) of the surface layers [Kononenko, 2005] as the surface graphitization was considered as one of lubrication mechanisms of DLC films [Liu et al., 1996; Konicek et al., 2012]. In case of ns-laser processing, the effect of surface graphitization on reducing the friction coefficient of hydrogen-free and hydrogenated DLC films was reported to be strongly pronounced on the micro and nanoscale [Ding et al., 2012; Roch et al., 2014; Komlenok et al., 2015; Komlenok et al., 2016]. Using friction force microscopy technique, the laser-produced graphitic layer was found to act as a solid lubricant during sliding of Si and diamond-coated tips on the DLC film surfaces [Komlenok et al., 2015; Komlenok et al., 2016]. It was also observed that the positive effect of the surface graphitization on friction could be reversed by nanoscale topography changes and enhanced surface roughness occurred as a result of laser-induced microspallations in diamond-like nanocomposite (DLN) films [Zavedeev et al., 2016].

For femtosecond-laser processing of DLC films, the role of surface modifications (graphitization, ripple formation) in the friction behaviour was reported to be ambiguous [Yasumaru et al., 2008; Pfeiffer et al., 2013], and the improved friction performance was observed only for certain friction pairs under high load sliding conditions during pin-on-disk tests [Pfeiffer et al., 2013]. Recently we found an interesting microfriction behaviour of laser-patterned DLN films which was characterized by strong influence of capillary forces on the friction forces under very low normal loads (tens of nanonewtons) and much lower friction forces on the laser-modified surface than on the original DLN film [Zavedeev et al., 2017]. In this paper, we focus on femtosecond-laser surface modification and micropatterning of DLN films under low-fluence multipulse irradiation, and on friction force microscopy study of laser-patterned films to get new data about the role of the surface modifications (graphitization, spallation, ablation, nanostructuring) in the improved friction properties.

2. Experimental

Diamond-like nanocomposite (a-C:H,Si:O) films were deposited on Si substrates using a plasma-assisted chemical vapor deposition from a polyphenylmethyl siloxane vapor [Dorfman, 1992]. The film thickness ranged from 2 to 3 μm . The film composition determined by electron probe micro-analysis was [C]=74-80%, [O]=9-12%, [Si]=11-14% at. The content of hydrogen was in the range of 0.1-0.4 of the atomic concentration of carbon, with the typical composition of DLN coatings being around $(\text{CH}_{0.15})_{0.7}(\text{SiO}_{0.4})_{0.3}$ [Dorfman, 1992; Scharf et al., 2007]. The hardness (H_{IT}) and Young's modulus (E_{IT}) of DNL films were measured by nanoindentation using a nanoindenter NHT2-TTX, CSM Instruments SA. Typical values of the nanohardness and elastic modulus were in the range of H_{IT} =22-28 GPa and (E_{IT})=135-190 GPa; the internal stresses in the films did not exceed the value of 250 MPa [Zavedeev et al., 2016].

Laser surface micropatterning of the DLN films was carried out using a 5W SATSUMA femtosecond laser (from Amplitude – Systèmes) generating pulses of τ =320 fs duration at the wavelength λ =1030 nm. The average power was varied from 100 to 1000 mW at the pulse repetition rate f = 101 kHz, corresponding to the range of the laser pulse energy (ϵ) from 1 to 10 μJ . The laser spot radius was w_0 = 21.4 μm , and the peak

fluence (E) in the spot center ranged from 0.14 to 1.4 J/cm². A high precision scanner was used to control the scanning beam velocities (V_s) from 10 m/s down to 0.05 m/s. The high scanning velocity (10 m/s) was applied for the single-pulse irradiation, while the low scanning velocities from 0.8 down to 0.05 m/s were used in the multipulse regime to vary the effective number of pulses from $N=5$ to 80. In the multipulse regime, periodic linear micropatterns were produced over the surface areas of 2×20 mm². The laser-patterned samples were examined using optical microscopy (OM) and atomic force microscopy (AFM). The structure modifications of the DLN films were studied using Raman spectroscopy (Ar-ion laser, excitation wavelength 514.5 nm).

The surface relief and friction properties of laser-patterned DLN films on the nano and microscale were studied with an atomic force microscope of the NTEGRA Spectra system (NT-MDT) using a lateral force mode (LFM). Si probes with the spring constant of 2 N/m and the tip radius of $R_{tip}=10$ nm and $R_{tip}=1.5$ μ m were used. The tip scanning speed was 80 μ m/s in the LFM measurements. The LFM measurements were carried out in ambient air at relative humidity RH=45-50% and room temperature $T=25^\circ$ C.

3. Results and Discussion

3.1. Femtosecond laser surface modification & micropatterning of DLN films

Laser interaction with hydrogenated DLC (a-C:H) films is characterized by three main processes – graphitization, spallation and evaporation (ablation), which were clearly pronounced in progressive changes of laser spot profiles with increasing pulse energy [Kononenko et al., 2005]. The laser damage of a-C:H films, starting from graphitization and spallation, was found to be alike for a wide range of pulse durations from nanoseconds to tens of femtoseconds [Kononenko et al., 2005; Ding et al., 2011; Bonse et al., 2013]. In our experiments, laser irradiation of DLN films with single pulses of 320-fs duration showed similar features of the surface damage (graphitization, spallation, evaporation) with increasing fluence, see Fig. 1. The threshold of fs-laser damage under single-pulse irradiation amounts to $E_{th}=0.35$ J/cm² (pulse energy $\epsilon_{th}=2.5$ μ J) at which the graphitization over the spot (swelling height of $h_s=50$ nm) and spallation in the spot center occurs simultaneously. The actual damage threshold is almost twice less the above value of E_{th} because of low light absorption in the DLN film at the laser wavelength.

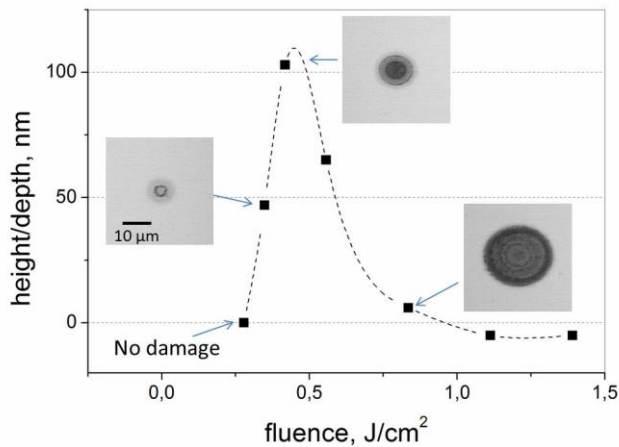


Fig. 1. Height/depth in the center of laser spots vs peak fluence during single-pulse irradiation of the DLN film (along with OM images of several spots); no damage is observed at the fluence $E=0.28$ J/cm².

From the spectral ellipsometry measurements the refractive index $n=2$ and absorption coefficient $\alpha=2.6 \cdot 10^3 \text{ cm}^{-1}$ (at $\lambda=1030 \text{ nm}$) are obtained, and simple estimations show that $\delta\epsilon_r=11\%$ of the incident pulse energy is reflected from the DLN surface, $\delta\epsilon_{ab}=43\%$ is absorbed in the DLN film (of $2.5 \mu\text{m}$ thickness), and $\delta\epsilon_{st}=46\%$ is transmitted to the Si substrate. At $E>E_{th}$ all the processes – surface graphitization, multilevel spallation and evaporation – develop gradually with laser fluence that leads to increasing spot size (see OM images in Fig. 1) and makes the laser patterning conditions (at high pulse energies) not suitable for micron-thick DLN coatings.

At the pulse energies below the laser damage threshold, at $\epsilon \leq 2 \mu\text{J}$, no spots were observable on the film surface after single-pulse irradiation. However the transition to the multipulse irradiation at the same pulse energy $\epsilon = 2 \mu\text{J}$ revealed an appearance of the surface relief changes attributed to progressive graphitization, microspallations, and developing ablation. AFM images in Fig. 2 show the evolution of the laser-irradiated surface in dependence on the scanning beam velocity and increasing number of pulses from $N=5$ to 20.

The beginning of fs-laser induced graphitization of the DLN surface is observed at the scanning speed $V_s=0.8 \text{ m/s}$ and $N=5$; the AFM image in Fig. 2a evidences a small swelling height ($h_s \sim 20 \text{ nm}$) of the spots at this stage. A criterion of the occurrence and growth of a graphitized surface layer during multipulse irradiation is the achievement of the graphitization temperature which ranges from 480 to 580 K for hydrogenated DLC and DLN films [Yang et al., 2003]. As discussed in our recent paper [Zavedeev et al., 2017], numerical calculations of the temperature and thickness of the laser-graphitized layer have evidenced (i) the achievement of the surface temperature sufficient for the beginning of graphitization (even for low light absorption in the films), and (ii) rapid growth of the graphitized layer assuming gradual increase of the absorption coefficient after each successive pulse action. This is consistent with the non-uniform surface swelling in Fig. 2a which results from multipulse irradiation at a given scanning speed. The distance between laser spots during the beam scanning at $V_s=0.8 \text{ m/s}$ and $f=101 \text{ kHz}$ is equal to $V_s/f \approx 8 \mu\text{m}$ and coincides with the distance between the positions of the maximum swelling heights along the non-uniformly graphitized strip. It means that the actions of four laser pulses lead to gradual increase of the light absorption in the surface layer and the action of the fifth pulse is mostly responsible for the observed surface swelling.

The increase of the absorption coefficient of the IR laser radiation and growth of the graphitized layer during multipulse irradiation are responsible for further temperature growth unless the evaporation starts. Figure 2b shows all the surface relief features caused by graphitization, spallation and incipient ablation occurred after ~ 10 laser shots in the laser-irradiated strip. Upon reaching the evaporation temperature, the laser ablation starts and the formation of periodic nanostructures on the graphitized surface develops (under irradiation with a linearly polarized laser beam) [Miyazaki and Miyaji, 2014], which is clearly observed in laser-irradiated strip in Fig. 2c.

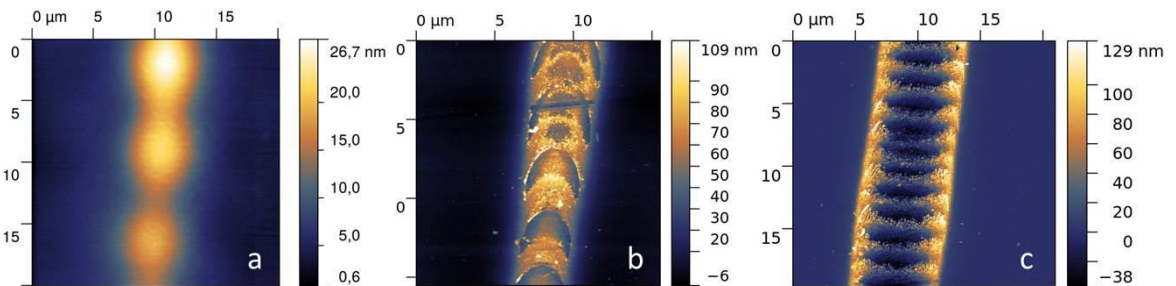


Fig. 2. AFM images of laser-irradiated regions formed during multipulse irradiation at the pulse energy $\epsilon=2 \mu\text{J}$ (fluence $E=0.28 \text{ J/cm}^2$) and different scanning beam velocities: (a) 0.8 m/s , (b) 0.4 m/s , and (c) 0.2 m/s .

In the experiments, the multipulse irradiation at $\epsilon=2 \mu\text{J}$ and $V_s=0.1$ to 0.05 m/s (pulse number $N\sim 40$ to 80) satisfy the conditions of the graphitization, developing ablation and surface nanostructuring, and they have been selected for micropatterning of the DLN film. As an example, Figure 3a shows a periodic linear micropattern consisting of graphitized strips of $9 \mu\text{m}$ width and $20 \mu\text{m}$ period fabricated on the DLN film for further testing of the friction properties on the micro and macroscale. The Raman spectra in Fig. 3b confirm the surface graphitization within the strip and also evidence that the film structure between the strips is identical to the original film.

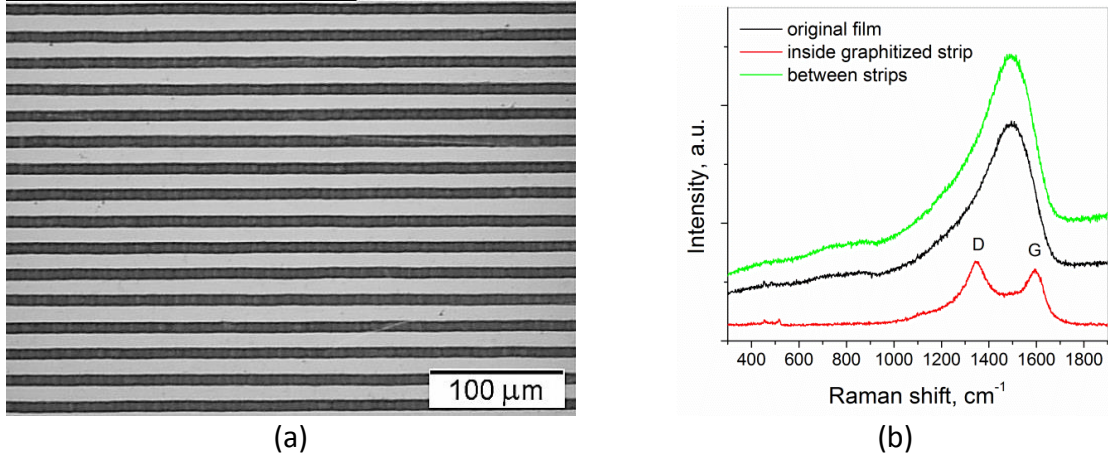


Fig. 3. (a) Periodic linear micropattern (graphitized strips of $<10 \mu\text{m}$ width and $20 \mu\text{m}$ period) fabricated on the DLN film surface during fs-laser multipulse irradiation at the pulse energy $\epsilon=2 \mu\text{J}$ (peak fluence $E=0.28 \text{ J/cm}^2$), and scanning beam velocity 0.05 m/s . (b) Raman spectra of the original film and laser-patterned region (inside the laser-irradiated strips and between the strips).

3.2. Friction force microscopy of laser-patterned DLN films

The LFM technique was applied to study (i) a single laser-graphitized strip fabricated under multipulse irradiation at $\epsilon=2 \mu\text{J}$ and $V_s=0.1 \text{ m/s}$ (fluence $E\sim 0.25 \text{ J/cm}^2$) and (ii) a laser micropattern (shown in Fig. 3a) fabricated at $\epsilon=2 \mu\text{J}$ and $V_s=0.05 \text{ m/s}$ (fluence $E=0.28 \text{ J/cm}^2$). The data of LFM examination of the laser-graphitized strip are presented in Fig. 4 which compares the friction images recorded with two Si tips of different radius ('sharp' tip of $R_{tip}=10 \text{ nm}$ and 'blunt' tip of $R_{tip}=1.5 \mu\text{m}$). The LFM measurements were made at very low loads on the tips: $F=24 \text{ nN}$ and $F=6 \text{ nN}$ for the sharp and blunt tips, respectively. In the friction images, the scale is given in the deflection angle of the cantilever (proportional to the friction force) so higher brightness of a local surface region corresponds to larger friction forces in that region.

Friction force (FF) images are obtained by subtraction of two lateral force (LF) images acquired during tip scanning from left to right and from right to left. This operation allows to significantly reduce the contribution of the surface relief slope to the LF signal. For a sharp tip, the laser-induced nanostructures are clearly visible in both the relief and friction images (Figs. 4a and 4b). The friction map is characterized by higher average level and friction force oscillations inside the graphitized strip compared to the original surface (Fig. 4b). The FF oscillations are due to high surface roughness inside the strip, so the subtraction of the 'forth and back' LF images does not compensate the effect of relief slope in the LF signal.

To overcome the 'high roughness' influence on the FF signal, the sharp tip has been intentionally blunted to obtain the tip of $R_{tip}=1.5 \mu\text{m}$ [Zavedeev et al., 2017]. Use of the blunt tip leads to smoothing of the nanostructured surface features (nano-ripples are not resolved). But most interestingly, the friction behavior

is strongly changed during LFM imaging with the blunt tip. The FF signal inside the laser-graphitized strip is found to be 1-2 orders of magnitude lower than that outside the strip on the film surface (Figs. 4c). In addition, a large difference is found between the force-distance curves for the blunt tip contacts inside and outside the strip (Fig. 5). For the sharp tip, the force-distance curves evidence (i) a lower stiffness of the graphitized material and (ii) a little difference between the pull-off forces on the original film ($F_{pull-off} \sim 9$ nN) and inside the strip ($F_{pull-off} \sim 6$ nN), see Fig. 5a. However, for the blunt tip the pull-off force is much higher on the original surface ($F_{pull-off} = 800$ nN) than that inside the strip ($F_{pull-off} = 12$ nN), see Fig. 5b.

It is known that in case of humid atmosphere, hydrophilic surfaces of the tip and the sample, and a large tip radius (hundreds nm and more), the predominant component of the pull-off force is the capillary force [Ando and Ino, 1998; Stifter et al., 2000]. This force is caused by the Laplace pressure in a water adsorbate meniscus formed between the tip and the film surface. For the original surface, its value can be obtained by the formula $F_{cap} = 2\pi R_{tip} \gamma (\cos \Theta_1 + \cos \Theta_2)$ [Ando and Ino, 1998], where R_{tip} is the tip radius, $\gamma = 72$ mN/m is the surface tension of water at 25°C, Θ_1 is the contact angle of water and original DLN surface, Θ_2 is the contact angle of water and Si tip. The value of $\Theta_1 = 73^\circ$ is taken for Si-DLC film from [Kalin and Polajnar, 2014], and the value of the contact angle between water and silicon is in the range of $\Theta_2 = 23^\circ$ to $\Theta_2 = 43^\circ$ [Ando and Ino, 1998]. For the blunt tip of $R_{tip} = 1.5 \mu\text{m}$, the above formula gives an estimation of the pull-off force $F_{pull-off} = 700 \div 820$ nN which is in good agreement with the measured pull-off force on the original surface.

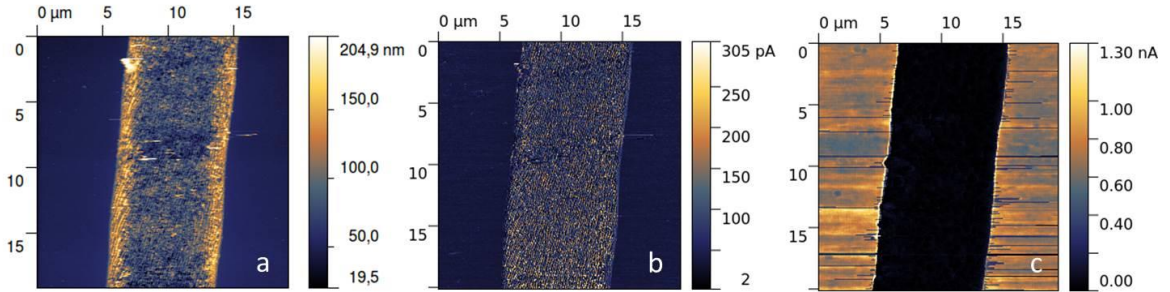


Fig. 4. Surface relief (a) and friction force (b,c) images of the laser-graphitized strip recorded with a sharp Si tip of $R_{tip} = 10$ nm at load on the tip $F = 24$ nN (a,b) and with a blunt Si tip of $R_{tip} = 1.5 \mu\text{m}$ at load $F = 6$ nN (c); the scale in friction images is given in the deflection angle of the cantilever [Zavedeev et al., 2017].

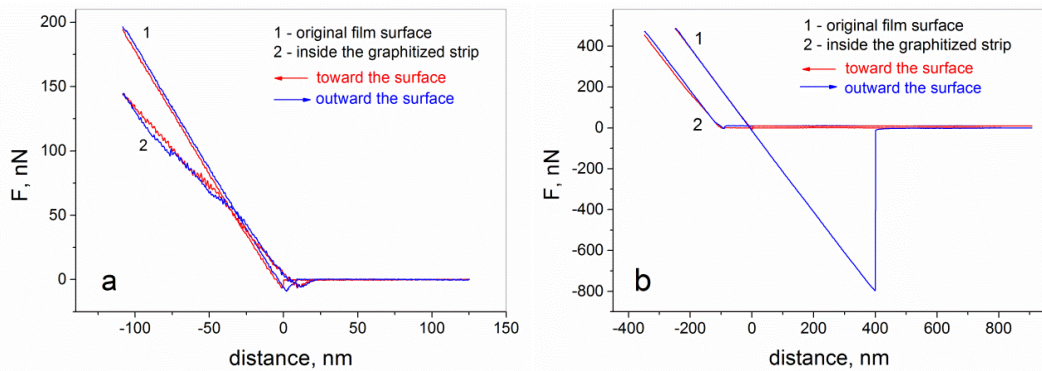


Fig. 5. Force-distance curves for the contacts of the sharp (a) and blunt (b) Si tips inside and outside the laser-graphitized strip (shown in Fig. 4); the curves 2 in (b) are shifted by 100 nm along the X axis for clarity.

According to the above estimates, the real load on the tip (on the original film) is increased by 700-800 nN due to the action of the capillary force. On the contrary, the value of the pull-off force on the strip indicates that the laser-modified material is hydrophobic and that total adhesion force does not exceed a few tens of nanonewtons in the laser-graphitized strips. So the observed decrease of the FF signal on the laser strip is caused mainly by the large difference between the real tip loads on the original and laser-modified surfaces.

The LFM examination of a laser micropattern (shown in Fig. 3a) was carried out with the blunt Si tip, and corresponding topography and friction force images are shown in Fig. 6. The difference between the irradiation conditions of the single strip (in Fig. 4) and micropattern (in Fig. 6) is mainly the twice lower scanning speed of the latter (and twice larger number of pulses) that leads to higher ablation depth of the strips and larger amount of the ablated and redeposited material around the strips. Indeed, the relief image of the micropattern (Fig. 6a) shows the strips of about 300 nm depth with nanostructured surface of the strip edges of a relatively large swelling height ($h_s \sim 100$ nm). The friction contrast between the original and patterned regions (in Fig. 6b) is clearly pronounced and can be characterized by the following distinctive features. Firstly, the friction is considerably lower in the laser-patterned region than on the original surface. Secondly, the reduced friction is observed also in unirradiated regions between the graphitized strips, with nanostructured swellings exhibiting higher friction than the surface between strips. Thirdly, the appearance of lower-friction areas in the tip scanning direction is observed on the original film (to the left of the pattern), that can be caused by transfer of a graphitic material from the laser-graphitized regions to the original surface, with these transferred particles acting as a lubricant.

It should be noted that the reduced friction in the laser-patterned region was accompanied with much lower pull-off forces than on the original film, similar to that shown in Fig. 5b. This means that the ablated and redeposited material is likely to change wettability of the film surface between the strips. The structure of the redeposited layer is not detectable by Raman spectroscopy (see Fig. 3b) because of its very small thickness. But the layer thickness is sufficient to enlarge hydrophobicity and improve microfriction between the strips. A particular structure of the redeposited layer is of interest and requires further investigations. The correlation between the graphitization degree and water contact angle of hydrogenated DLC films was reported [Lee et al., 2007], so the role of the surface graphitization seems to be more significant than that of nanostructuring in the enlarged hydrophobicity of the DLN surface.

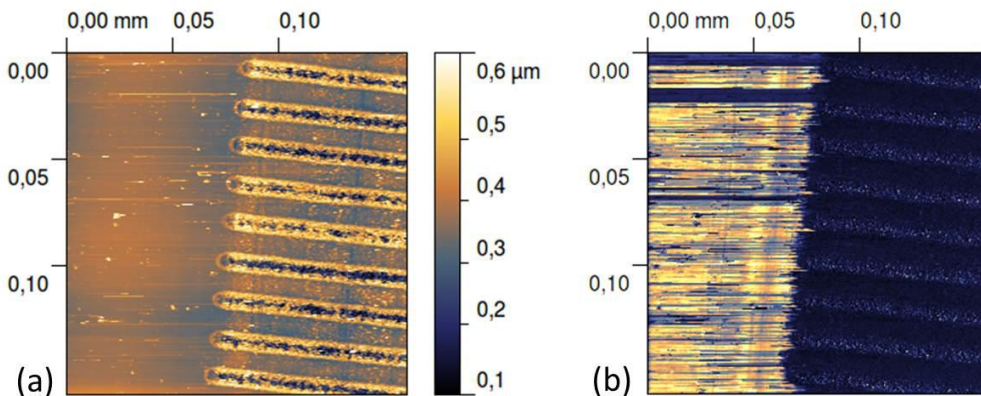


Fig. 6. Surface relief (a) and friction force (b) images (recorded with a blunt Si tip of $R_{tip}=1.5 \mu\text{m}$ at load $F=64$ nN) of the periodic linear micropattern fabricated on the DLN film surface during multipulse irradiation at the pulse energy $\epsilon=2 \mu\text{J}$ (fluence $E=0.28 \text{ J/cm}^2$) and scanning beam velocity 0.05 m/s.

4. Summary

Characteristic features of femtosecond-laser interaction with DLN films, surface modification and micropatterning of the films have been studied, aimed at modification and control of the frictional properties of laser-micropatterned DLN films on the nano and microscale. Regimes of low-fluence multipulse irradiation with IR femtosecond laser (1030 nm wavelength, 320 fs pulse duration, 101 kHz frequency) have been developed for producing periodic linear micropatterns (laser-graphitized strips) on the DLN films with the strip width significantly lower than the laser spot diameter.

Frictional properties of periodic linear micropatterns have been studied using lateral force microscopy technique. The LFM examinations with nano- and micro-sized Si tips (tip radius of 10 nm and 1.5 μm) have revealed considerable differences in the friction behavior of the laser-patterned film under very light loads and demonstrated much lower friction forces within laser-graphitized strips than on the original film. These findings result from enlarged hydrophobicity of laser-graphitized surface and strong influence of capillary forces of adsorbed water layers on friction under the 'nano' loads.

The preliminary analysis of the role of fs-laser-induced surface modifications (graphitization, spallation, ablation, nanostructuring) in the improved microfriction behaviour shows the main contribution of the graphitization and redeposition of ablated material in the enlarged hydrophobicity of the DLN surface. The structure of the redeposited layer and mechanism of the surface functionalization to improve microfriction properties of the DLN films are of interest and require further investigations.

Acknowledgements

The work was supported by the Russian Science Foundation under project No. 15-12-00039.

References

- Ando, Y., Ino, J., 1998. Friction and pull-off forces on submicron-size asperities, *Wear* 216, p. 115.
- Bonse, J., Hertwig, A., Koter, R., Weise, M., Beck, U., Reinstädt, P., Griepentrog, M., Krüger, J., Picquart, M., Haro-Poniatowski, E., 2013. Femtosecond laser pulse irradiation effects on thin hydrogenated amorphous carbon layers, *Applied Physics A* 112, p. 9.
- Ding, Q., Wang, L., Hua, L., Hu, T., Wang, Y., 2012. The pairing-dependent effects of laser surface texturing on micro tribological behavior of amorphous carbon film, *Wear* 274–275, p. 43.
- Ding, Q., Wang, L., Hu, L., Hu, T., Wang, Y., Zhang, Y., 2011. An explanation for laser-induced spallation effect in a-C:H films: altered phase evolution route caused by hydrogen doping, *Journal of Applied Physics* 109, p. 013501.
- Dorfman, V.F., 1992. Diamond-like nanocomposites (DLN), *Thin Solid Films* 212, p. 267.
- Etsion, I., 2005. State of the art in laser surface texturing, *J. Tribol.: Trans. ASME* 127, p. 248. Konov, V.I., 2012. Laser in micro and nanoprocessing of diamond materials, *Laser & Photonics Reviews* 6, p. 739.
- Kalin, M., Polajnar, M., 2014. The wetting of steel, DLC coatings, ceramics and polymers with oils and water: The importance and correlations of surface energy, surface tension, contact angle and spreading, *Applied Surface Science* 293, p. 97.
- Komlenok, M.S., Arutyunyan, N.R., Kononenko, V.V., Zavedeev, E.V., Frolov, V.D., Chouprik, A.A., Baturin, A.S., Scheibe, H.-J., Pimenov, S.M., 2016. Structure and friction properties of laser-patterned amorphous carbon films, *Diamond & Related Materials* 65, p. 69.
- Komlenok, M.S., Kononenko, V.V., Zavedeev, E.V., Frolov, V.D., Arutyunyan, N.R., Chouprik, A.A., Baturin, A.S., Scheibe, H.-J., Shupegin, M.L., Pimenov, S.M., 2015. Laser surface graphitization to control friction of diamond-like carbon coatings, *Applied Physics A* 121, p. 1031.
- Konicek, A.R., Grierson, D.S., Sumant, A.V., Friedmann, T.A., Sullivan, J.P., Gilbert, P.U.P.A., Sawyer, W.G., Carpick, R.W., 2012. Influence of surface passivation on the friction and wear behavior of ultrananocrystalline diamond and tetrahedral amorphous carbon thin films, *Physical Review B* 85, p. 155448.
- Kononenko, T.V., Kononenko, V.V., Pimenov, S.M., Zavedeev, E.V., Konov, V.I., Romano, V., Dumitru, G., 2005. Effects of pulse duration in laser processing of diamond-like carbon films, *Diamond & Related Materials* 14, p. 1368.

- Lee, S.C., Tai, F.C., Wei, C.H., 2007. Correlation between sp²/sp³ ratio or hydrogen content and water contact angle in hydrogenated DLC film, *Materials Transactions* 48, p. 2534.
- Liu, Y., Erdemir, A., Meletis, E.I., 1996. An investigation of the relationship between graphitization and frictional behavior of DLC coatings, *Surface & Coatings Technology* 86-87, p. 564.
- Miyazaki, K., Miyaji, G., 2014. Mechanism and control of periodic surface nanostructure formation with femtosecond laser pulses, *Applied Physics A* 114, p. 177.
- Mottay, E., Liu, X., Zhang, H., Mazur, E., Sanatinia, R., Pflöging, W., 2016. Industrial applications of ultrafast laser processing, *MRS Bulletin* 41, p. 984.
- Pfeiffer, M., Engel, A., Gruettner, H., Guenther, K., Marquardt, F., Reisse, G., Weissmantel, S., 2013. Ripple formation in various metals and super-hard tetrahedral amorphous carbon films in consequence of femtosecond laser irradiation, *Applied Physics A* 110, p. 655.
- Roch, T., Klein, F., Guenther, K., Roch, A., Mühl, T., Lasagni, A., 2014. Laser interference induced nano-crystallized surface swellings of amorphous carbon for advanced micro tribology, *Materials Research Express* 1, p. 035042.
- Scharf, T.W., Ohlhausen, J.A., Tallant, D.R., Prasad, S.V., 2007. Mechanisms of friction in diamondlike nanocomposite coatings, *Journal of Applied Physics* 101, p. 063521.
- Stifter, T., Marti, O., Bhushan, B., 2000. Theoretical investigation of the distance dependence of capillary and van der Waals forces in scanning force microscopy, *Physical Review B* 62, p. 13667.
- Yang, W.J., Choa, Y.H., Sekino, T., Shim, K.B., Niihara, K., Auh, K.H., 2003. Thermal stability evaluation of diamond-like nanocomposite coatings, *Thin Solid Films* 434, p. 49.
- Yasumaru, N., Miyazaki, K., Kiuchi, J., 2008. Control of tribological properties of diamond-like carbon films with femtosecond-laser-induced nanostructuring, *Applied Surface Science* 254, p. 2364.
- Zavedeev, E.V., Zilova, O.S., Barinov, A.D., Shupegin, M.L., Arutyunyan, N.R., Jaeggi, B., Neuenschwander, B., Pimenov, S.M., 2017. Femtosecond laser microstructuring of diamond-like nanocomposite films, *Diamond & Related Materials* 74, p. 45.
- Zavedeev, E.V., Zilova, O.S., Shupegin, M.L., Barinov, A.D., Arutyunyan, N.R., Roch, T., Pimenov, S.M., 2016. Effects of UV laser micropatterning on frictional performance of diamond-like nanocomposite films, *Applied Physics A* 122, p. 961.